ELSEVIER

Computer Aided Geometric Design 15 (1998) 165–186

COMPUTER AIDED GEOMETRIC DESIGN

Applications of Laguerre geometry in CAGD

Helmut Pottmann *, Martin Peternell

Institut für Geometrie, Technische Universität Wien, Wiedner Hauptstrasse 8–10, A-1040 Vienna, Austria

Received May 1996; revised April 1997

Abstract

We briefly introduce to the basics of Laguerre geometry and then show that this classical sphere geometry can be applied to solve various problems in geometric design. In the present part, we focus on applications of the cyclographic model of Laguerre geometry and the cyclographic map. It relates the medial axis and Voronoi curves/surfaces to special surface/surface intersections and the corresponding trimming procedures to hidden line removal. Rational canal surfaces are treated as cyclographic images of rational curves in $\mathbb{R}^4$. This leads to a simple control structure for rational canal surfaces. Its practical use is demonstrated at hand of modeling techniques with Dupin cyclides.

Keywords: Laguerre geometry; NC milling; Blending; Canal surface; Dupin cyclide; Geometrical optics; Medial axis; Rational curve; Rational surface; Voronoi curve; Voronoi surface

Introduction

Laguerre geometry is a classical sphere geometry that has its origin in the work of the French mathematician E. Laguerre (1834–1886). It is based on oriented spheres, oriented hyperplanes and oriented contact between them. There is an extensive classical literature on this kind of geometry (see, for example (Blaschke, 1929; Müller and Krames, 1929)). Laguerre geometry is also an active area within modern geometry (see (Benz, 1992; Cecil, 1992)). In this paper, we will point to a new facet of Laguerre geometry, namely its role in geometric design. It turns out that several geometric design problems can be solved in a surprisingly simple way if one uses Laguerre geometry. We continue these studies in (Peternell and Pottmann, 1997a).

* Corresponding author. E-mail: pottmann@geometrie.tuwien.ac.at.

0167-8396/98/$19.00
PII S0167-8396(97)00023-X

In a brief tutorial on Laguerre geometry we describe those fundamentals necessary for our geometric design applications. The cyclographic model of Laguerre geometry and the cyclographic map lead us quite naturally to known applications such as the medial axis and closely related concepts (bisectors, Voronoi surfaces) and geometrical optics. Furthermore, it suggests the introduction of a simple control structure for rational canal surfaces. Its use is demonstrated at hand of algorithms for modeling with Dupin cyclides. The efficiency of this new approach to Dupin cyclides in CAGD is based on the fact that cyclides are cyclographic images of circles in a pseudoeuclidean (pe) metric. The relatively simple transfer of results on euclidean circular splines to pe geometry then yields techniques to model more complicated canal surfaces from cyclide pieces. As an example, we study double-cyclide blends with help of pe biarcs.

1. Fundamentals of Laguerre geometry

1.1. Euclidean Laguerre space

The fundamental elements of Laguerre geometry in euclidean $\mathbb{R}^n$ are *oriented hyperplanes* and *cycles*. A cycle is an oriented sphere or a point (sphere with radius 0). The orientation is determined by a unit normal vector field or equivalently by a signed radius in the case of the sphere. The applications given later belong to the cases $n = 2, 3$.

The basic relation in Laguerre geometry is that of *oriented contact of cycle and or. hyperplane*. An oriented sphere and an or. hyperplane are in oriented contact, if they are tangent and the unit normals coincide at the point of contact. For a point and an or. hyperplane, oriented contact equals incidence. When no ambiguity can arise, or. hyperplanes will simply be called hyperplanes.

Laguerre geometry studies properties which are invariant under Laguerre transformations. A *Laguerre transformation* consists of two bijective maps, one in the set of cycles and the other one in the set of hyperplanes. Additionally, a Laguerre transformation preserves oriented contact and noncontact between cycles and hyperplanes. A simple example of a Laguerre transformation is a *dilatation* which adds a constant $d \neq 0$ to the signed radius of each cycle and leaves its midpoint unchanged. Note that this map does not preserve points. Considering a hypersurface as envelope of its oriented tangent hyperplanes, a dilatation maps the surface onto its offset at distance d. This already indicates the advantage of using Laguerre geometry in connection with offsets.

Using cartesian coordinates x_i in $\mathbb{R}^n$, each hyperplane e is defined by a linear equation

$$e_0 + e_1 x_1 + \cdots + e_n x_n = 0.$$

The coefficients e_i are called hyperplane coordinates of e. The normal vector $(e_1, \ldots, e_n)$ defines the orientation of the hyperplane and is always assumed to be normalized, $e_1^2 + \cdots + e_n^2 = 1$.

The model of Laguerre geometry we have just described is also referred to as *standard model*.

1.2. The cyclographic model

Embedding $\mathbb{R}^n$ in $\mathbb{R}^{n+1}$ as hyperplane $x_{n+1} = 0$, we map each or. hyperplane e to the hyperplane $E = \zeta^*(e)$, defined by the homogeneous coordinates

$$E = (e_0, \ldots, e_n, 1). \tag{1}$$

Note that the euclidean angle of E and $\mathbb{R}^n$ equals $\gamma = \pi/4$; hence, we refer to E as a γ-hyperplane. A cycle C with midpoint m and signed radius r is represented by the point $\zeta(C) := (m_1, \ldots, m_n, r)$ in $\mathbb{R}^{n+1}$. Note that $\zeta(C)$ is determined by ζ^* if C is interpreted as set of or. tangent hyperplanes. Those hyperplanes e have images $\zeta^*(e)$ that pass through $\zeta(C)$; all these hyperplanes $\zeta^*(e)$ form the tangent hyperplanes of a quadratic cone $\Gamma(x)$ with vertex $x = \zeta(C)$. Its generators form the angle γ with $\mathbb{R}^n$; such lines will be called γ-lines henceforth. In other words, $\Gamma(x)$ intersects the ideal plane in the quadric Ω with equations $p_0 = 0$, $p_1^2 + \cdots + p_n^2 - p_{n+1}^2 = 0$. Here, $(p_0, \ldots, p_{n+1})$ are homogeneous coordinates related to the affine coordinates x_i by $x_i = p_i/p_0$. The obtained $(n+1)$-dimensional model of n-dimensional Laguerre geometry is called *cyclographic model*. The low dimensional case $n = 2$ is illustrated in Fig. 1.

In the cyclographic model, Laguerre transformations are special affine maps. In the projective extension, they map the quadric at infinity Ω onto itself. Interpreting Ω as absolute quadric in a *pseudoeuclidean* (pe) metric, Laguerre transformations are *pe similarities* of the form

$$x' = a + \lambda A \cdot x \tag{2}$$

with a constant $\lambda \neq 0$ and a pe orthogonal matrix A. It satisfies

$$A^{\mathrm{T}} \cdot E_{pe} \cdot A = E_{pe}, \tag{3}$$

where E_{pe} is a diagonal matrix with $e_{1,1} = \cdots = e_{n,n} = 1$, $e_{n+1,n+1} = -1$. We will also use the *pe scalar product* of two vectors, $\langle a, b\rangle_{pe} := a^{\mathrm{T}} \cdot E_{pe} \cdot b$. The space $\mathbb{R}^{n+1}$ with

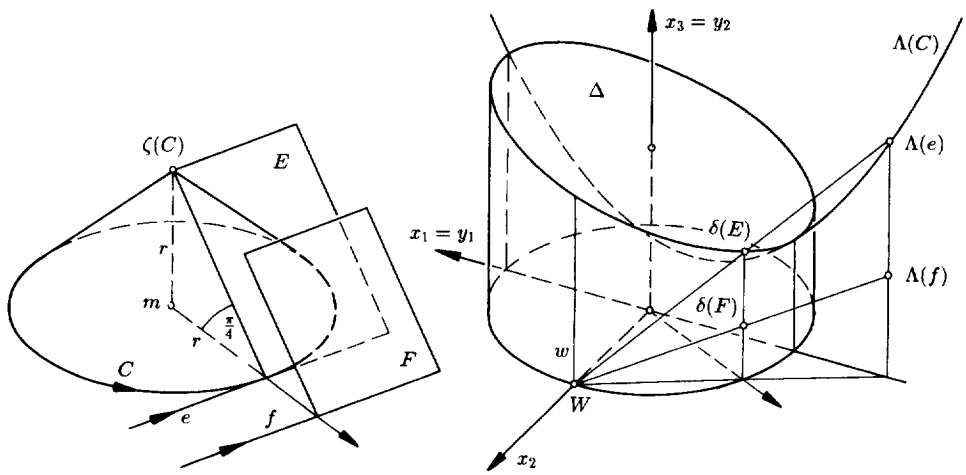

Fig. 1. Models of euclidean Laguerre geometry.

this scalar product is often denoted by *Lorentz space*. A vector a is said to be *timelike*, *lightlike* or *spacelike*, respectively, depending on whether $\langle a,a\rangle_{pe}$ is negative, zero or positive. A line with direction vector a is called *elliptic*, if a is timelike. The angle between the line and $\mathbb{R}^n$ exceeds $\gamma = \pi/4$. A γ-line or *parabolic* line is defined by a lightlike direction vector and a line with spacelike direction vector is called a *hyperbolic* line.

Consider two points $a = \zeta(A)$ and $b = \zeta(B)$ in $\mathbb{R}^{n+1}$ on a hyperbolic line. Then, any common tangent hyperplane of the two cycles A, B touches the cycles at points with euclidean distance $d = \sqrt{\langle a-b, a-b\rangle_{pe}}$. The *tangential distance* d of the two cycles is the *pe distance* of the image points a, b in $\mathbb{R}^{n+1}$. For two points on a parabolic line, we get $d = 0$ and the corresponding cycles A, B are tangent. On elliptic lines, one may use the invariant $d^2 < 0$ of two points. *Pe congruences* in $\mathbb{R}^{n+1}$ (described by (2) with $|\lambda| = 1$) preserve the squared pe distance of any two points and correspond to tangential distance preserving Laguerre transformations in $\mathbb{R}^n$.

Further models of euclidean Laguerre geometry shall be discussed. These are useful for the treatment of rational curves and surfaces with rational offsets (Peternell and Pottmann, 1997a).

1.3. The Blaschke model

If more emphasis is on or. hyperplanes rather than cycles, one might be interested in a model where or. hyperplanes appear as points. This can easily be done by applying a duality $\delta : \mathbb{R}^{n+1*} \to \mathbb{R}^{n+1}$ (Blaschke map),

$$\delta(E) = (1, e_1, \ldots, e_n, e_0). \tag{4}$$

The set of hyperplanes E is mapped to points contained in a hypercylinder $\Delta \subset \mathbb{R}^{n+1}$ with equation Δ: $x_1^2 + \cdots + x_n^2 = 1$. In this *Blaschke model*, cycles (as sets of or. tangent hyperplanes) appear as hyperplanar cuts of Δ (see Fig. 1). Laguerre transformations are seen as projective maps which preserve Δ. Parallel oriented hyperplanes of the standard model are represented as points in the same generator (parallel to the x_{n+1}-axis) of Δ.

1.4. The isotropic model

Finally, we obtain an affine space (appropriately extended) as model of Laguerre space. For that, let w be the generator line of Δ containing the point $W(0,\ldots,0,1,0)$. Furthermore, let $\bar{\mathbb{R}}^n$ be the hyperplane $x_n = 0$ in $\mathbb{R}^{n+1}$, parallel to w; we use coordinate functions $y_1 = x_1, \ldots, y_{n-1} = x_{n-1}$, $y_n = x_{n+1}$ in it. Applying the 'stereographic' projection $\sigma : \Delta - w \to \bar{\mathbb{R}}^n$ with center W to the cylindrical model, we get a map from or. hyperplanes e with unit normal $\neq (0,\ldots,0,1)$ to points in $\bar{\mathbb{R}}^n$ via

$$\sigma \circ \delta \circ \zeta^*(e) = \frac{1}{1-e_n}(e_1, \ldots, e_{n-1}, e_0). \tag{5}$$

Interpreting cycles as sets of tangent hyperplanes, we may state an important well-known result that can be proved by straightforward calculation (see Fig. 1).

Lemma 1.1. *The set of tangent hyperplanes of a cycle Σ is mapped with $\sigma \circ \delta \circ \zeta^*$ to the set of points of a paraboloid of revolution or a hyperplane Ψ satisfying*

$$\Psi\colon\ 2y_n + (y_1^2 + \cdots + y_{n-1}^2)(r + m_n) + 2y_1 m_1 + \cdots + 2y_{n-1}m_{n-1} + r - m_n = 0. \tag{6}$$

So far, or. hyperplanes in $\mathbb{R}^n$ with unit normal $(0,\ldots,0,1)$ do not have an image point in $\bar{\mathbb{R}}^n$. One therefore forms the so-called isotropic conformal closure $I^n := \bar{\mathbb{R}}^n \cup \mathbb{R}$ of $\bar{\mathbb{R}}^n$ and an extended map

$$\Lambda := \bar{\sigma} \circ \delta \circ \zeta^*,$$

which maps the or. hyperplane $(e_0, 0, \ldots, 0, 1) \subset \mathbb{R}^n$ onto the real number e_0. To fix the problem of missing images of exceptional or. hyperplanes in Lemma 1.1, we have to extend the paraboloids Ψ by $r + m_n$, which equals 0 for a hyperplane Ψ. The resulting model of Laguerre space, where or. hyperplanes are represented as points and cycles appear as paraboloids or hyperplanes (called *isotropic spheres*), is called *isotropic model*. Very important for our applications in (Peternell and Pottmann, 1997a) is the transformation Λ which describes the change from the standard model to the isotropic model.

In I^n, y_n-parallel lines (called *isotropic lines*) represent parallel or. hyperplanes of the standard model. For simplicity, let us now restrict to $n = 3$. In I^3, nonisotropic lines as well as ellipses, whose normal projection onto $y_3 = 0$ are circles, and parabolas with isotropic axis are called *isotropic Möbius circles*. They may be obtained as intersection of 2 surfaces (6). Therefore, they are the Λ-image of the common tangent planes of 2 cycles, i.e., the planes of a pencil or the tangent planes of a cone or cylinder of revolution. This also shows that isotropic (y_3-parallel) planes as well as isotropic cylinders with a circular cross section in $y_3 = 0$ represent planes parallel to the planes of a pencil or to the tangent planes of a cone of revolution.

In the isotropic model, Laguerre transformations are realized as special quadratic transformations, so-called *isotropic Möbius transformations*. Let us consider two special cases. A translation in the standard model, represented in hyperplane coordinates by

$$(e_0, \ldots, e_n) \mapsto (e_0 + a_1 e_1 + \cdots + a_n e_n, e_1, \ldots, e_n)$$

yields in I^n the transformation

$$(y_1, \ldots, y_n) \mapsto \Big(y_1, \ldots, y_{n-1}, y_n + a_1 y_1 + \cdots + a_{n-1} y_{n-1} + \frac{a_n}{2}\big(y_1^2 + \cdots + y_{n-1}^2 - 1\big)\Big). \tag{7}$$

A dilatation $(e_0, \ldots, e_n) \mapsto (e_0 + d, e_1, \ldots, e_n)$ appears as isotropic Möbius transformation

$$(y_1, \ldots, y_n) \mapsto \Big(y_1, \ldots, y_{n-1}, y_n + \frac{d}{2}\big(y_1^2 + \cdots + y_{n-1}^2 + 1\big)\Big). \tag{8}$$

1.5. A dual isotropic model

We pick a fixed oriented hyperplane a in $\mathbb{R}^n$, say $x_n = 0$ with normal $(0,\dots,0,1)$. An arbitrary or. hyperplane e determines a γ-hyperplane $E = \zeta^*(e) = (e_0,\dots,e_n,1)$. Its intersection with $\zeta^*(a) = (0,\dots,0,1,1)$ is now projected orthogonally onto $\mathbb{R}^n$ and yields a (non oriented) hyperplane

$$\Lambda^*(e) = (e_0,\dots,e_{n-1},e_n - 1). \tag{9}$$

It is the euclidean bisector of e and the fixed or. hyperplane a, i.e., the locus of points possessing the same signed distance to e and a. Currently, a has no image and the remaining or. hyperplanes parallel to a are mapped to the hyperplane at infinity, which shows that the projective closure is not the right one for the image space. In fact, Λ^* generates a *dual isotropic model*. To convert to the previous isotropic model, we apply the polarity π with respect to the isotropic sphere

$$y_1^2 + \cdots + y_{n-1}^2 - 2y_n = 0.$$

$\Lambda^*(e)$ is mapped to the point with inhomogeneous coordinates

$$\pi \circ \Lambda^*(e) = \frac{1}{1-e_n}(e_1,\dots,e_{n-1},-e_0).$$

Up to a reflection at $y_n = 0$, we get exactly $\Lambda(e)$ as in (5). Hence, we can deduce the properties of the present dual isotropic model from the isotropic model.

Concerning applications discussed in (Peternell and Pottmann, 1997a), the inverse transformation $(\Lambda^*)^{-1}$ is of particular interest. Taking the normalization $e_1^2 + \cdots + e_n^2 = 1$ in (9) into account, we find with nonnormalized homogeneous coordinates $(y_0,y_1,\dots,y_n)$ of the hyperplane y to be transformed,

$$(\Lambda^*)^{-1}(y) = \left(y_0,\dots,y_{n-1},\frac{y_n^2 - y_1^2 - \cdots - y_{n-1}^2}{2y_n}\right). \tag{10}$$

For more details on Laguerre geometry and its relation to Einstein's theory of special relativity, we refer the reader to Benz (1992), Blaschke (1929) and Cecil (1992).

2. Cyclographic mapping of curves and surfaces

The mapping $c := \zeta^{-1}$ maps any point $x = (x_1,\dots,x_{n+1})$ in $\mathbb{R}^{n+1}$ to a cycle in $\mathbb{R}^n$ with center $(x_1,\dots,x_n)$ and radius x_{n+1}.

Connected to c is the map $c^* := (\zeta^*)^{-1}$ from the set of γ-hyperplanes in $\mathbb{R}^{n+1}$ to oriented hyperplanes in $\mathbb{R}^n$. A point $x \in E \subset \mathbb{R}^{n+1}$ is mapped onto a cycle $c(x)$ touching $c^*(E)$. The pair (c,c^*) is called *cyclographic map*. A detailed study of this beautiful part of classical geometry (mostly for $n = 2$) may be found in the monograph on the cyclographic map by Müller and Krames (1929).

Here, we will present a short tutorial on the cyclographic map and show that its application to curves in $\mathbb{R}^3$ and surfaces in $\mathbb{R}^4$ provides a useful framework for dealing with the medial axis and related concepts (see also (Hoffmann, 1992)). As a byproduct,

we obtain a well-known relation to certain problems in geometrical optics. Applying the cyclographic map to curves in $\mathbb{R}^4$ yields a simple approach to the design of canal surfaces, particularly to those composed of Dupin cyclides.

2.1. *Cyclographic mapping of curves in* $\mathbb{R}^3$

Let $p(t)$ be a real C^1 curve $\subset \mathbb{R}^3$. With help of the cyclographic map c we get a one parameter set of cycles $c(p(t))$ whose envelope $c(p)$ is called the cyclographic image of the curve p.

First we discuss the image of a line p. For a hyperbolic line p, $c(p)$ contains two real (oriented) lines $c(p)_1 = t_1$, $c(p)_2 = t_2$. For each $x \in p$ the lines t_1, t_2 are tangent to the cycle $c(x)$ at points x_1, x_2. We call the oriented line elements (x_1, t_1) and (x_2, t_2) the *cyclographic image of the line element* (x, p). The lines xx_1, xx_2 are generators of the γ-cone $\Gamma(x)$ with vertex x (see Fig. 2). In other words: t_1 and t_2 are the intersections of the γ-planes through p with the reference plane $\mathbb{R}^2$.

If p is a γ-line, all image cycles of points in p possess a common oriented line element (x, t_1), where x ist the intersection of p and $\mathbb{R}^2$. Thus, points a, b on the same γ-line are mapped onto tangent cycles $c(a), c(b)$. An elliptic line p has no real image curve $c(p)$.

For a general curve p, we proceed as above and map its line elements (p, t), where t is the tangent $p + \lambda\dot{p}$ (Fig. 1).

Let us first consider the case of a curve p all whose tangents are γ-lines. Such a curve (called *γ-curve*) has constant slope $\gamma = \pi/4$ against $\mathbb{R}^2$. Its tangent surface $T(p)$ is a developable surface whose tangent planes (=osculating planes of the line of regression p) also form the constant angle γ with $\mathbb{R}^2$. We call $T(p)$ a *γ-developable*. Any line element of p has one oriented line element as cyclographic image. These line elements touch the image curve $c(p)$ which is the intersection of $T(p)$ with $\mathbb{R}^2$. The image cycles $c(x)$ of points $x \in p$ are oriented osculating circles of $c(p)$. Hence, the evolute of $c(p)$ is the orthogonal projection p' (top view) of p onto $\mathbb{R}^2$. The tangent surface $T(p)$ itself

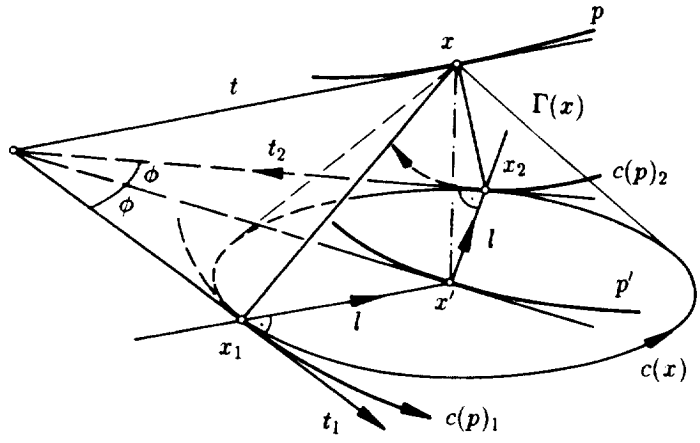

Fig. 2. Cyclographic image of a curve and optical interpretation.

is the cyclographic preimage of all cycles tangent to the oriented curve $c(p)$, or in other words, it is the graph of the signed distance function to the curve $c(p)$.

The cyclographic mapping of general curves may be described as follows. *The cyclographic image $c(p)$ of a C^1 curve $p(t) \subset \mathbb{R}^3$ is the intersection of the γ-developables passing through $p(t)$ with the reference plane $\mathbb{R}^2$. For a curve p with only hyperbolic tangents, $c(p)$ contains 2 components, a γ-curve is mapped to a single curve $c(p)$ and a curve with only elliptic tangents possesses no real image.*

We summarize some important facts on the cyclographic image $c(p)$ (compare (Müller and Krames, 1929)).

(1) Let $t_0 \in \mathbb{R}$ be an isolated zero of $\langle \dot{p}(t_0), \dot{p}(t_0) \rangle_{pe}$, i.e., $p(t_0)$ has a γ-tangent and separates a hyperbolic curve segment from an elliptic one (see b in Fig. 3). Then $p(t_0)_1 = p(t_0)_2$ is a vertex of $c(p)$ and the cycle $c(p(t_0))$ has contact of order 3 with $c(p)$ at $p(t_0)_1 = p(t_0)_2$. The image curve $c(p)$ can have more vertices than these.

(2) If $p(t)$ possesses an inflection point at $t = t_0$, then $c(p)$ has inflection points at $p(t_0)_1 = p(t_0)_2$.

(3) If $t_0 \in \mathbb{R}$ is an isolated zero of $p_3(t)$, then $p(t_0)_1 = p(t_0)_2$ is a double point of $c(p)$. Especially if $\dot{p}(t_0) \perp \mathbb{R}^2$, $c(p(t_0))$ is a focal point of $c(p)$ (see Fig. 3) in the sense of J. Plücker (intersection of tangents through the circular points).

(4) Let p be an algebraic curve with rank r (which is defined as the order of its tangent surface $T(p)$). If g is the number of common tangents of $p(t)$ and the pe absolute conic Ω in the ideal plane of $\mathbb{R}^3$, then $2r - g$ is the algebraic class of the γ-developable through p and therefore the class of $c(p)$. For more details and other algebraic characteristics, see (Müller and Krames, 1929).

Example 2.1. Consider an ellipse or hyperbola p,

$$x_1 = 0, \quad ax_2^2 + bx_3^2 = 1,$$

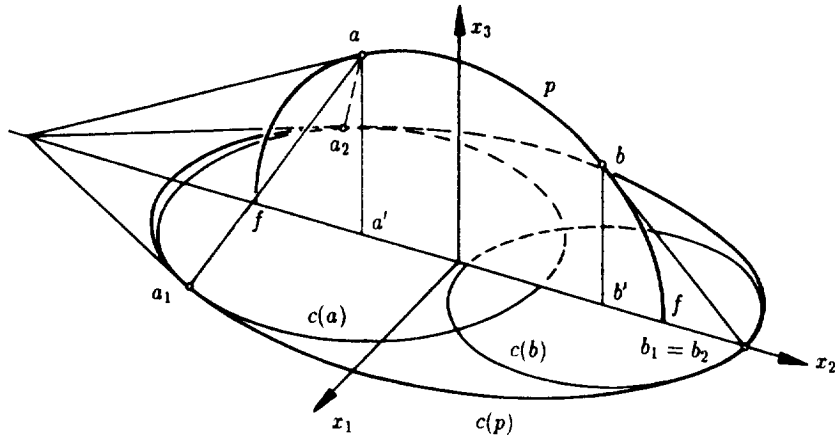

Fig. 3. Cyclographic image of a conic.

symmetric with respect to the reference plane $\mathbb{R}^2$. Without any computation, it is easy to derive the image curve. As rank of a planar curve we have to take its class, which is 2 in our case. There are no common tangents with Ω and thus the γ-developable $\Gamma(p)$ through p is of class 4. Like p, it is also symmetric with respect to $\mathbb{R}^2$. The angle of $\Gamma(p)$ and $\mathbb{R}^2$ equals γ and the intersection $c(p) = \Gamma(p) \cap \mathbb{R}^2$ is a double curve, hence of class 2. Thus, $c(p)$ must be a (not necessarily real) *conic*. The intersection points of p with $\mathbb{R}^2$ are focal points and the γ-tangents of p intersect $\mathbb{R}^2$ at vertices of $c(p)$ (see Fig. 3).

An important special case occurs, if p is a *pe circle*, that is a conic whose points at infinity lie in Ω. Such curves are planar intersections of γ-cones. For any pe circle p, the surface $\Gamma(p)$ splits into two γ-cones (one of which degenerates to a γ-plane if p is a parabola). Hence, the cyclographic image is formed of two cycles, or it consists of a cycle and an oriented line for a parabolic pe circle p. In our symmetric case (to $a = -b$), $c(p)$ consists of two points; the cycles $c(x)$ to $x \in p$ form an elliptic or hyperbolic pencil for a pe circle with hyperbolic or elliptic tangents, respectively.

Intersecting $\Gamma(p)$ with a plane parallel to $\mathbb{R}^2$ and projecting it into $\mathbb{R}^2$, we obtain an offset of $c(p)$. The offset is algebraic of class 4, but not rational, if p is not a pe circle. This follows from the fact that $\Gamma(p)$ is not rational. It is well known that a developable of class 4 connecting 2 conics is rational if and only if it possesses a double tangent plane (dual to the rationality of quartics of the first kind with a double point). Since any ellipse (different from a circle) and any hyperbola may appear as cyclographic image $c(p)$ of a conic p, *the offsets of these conics are never rational.*

Example 2.2. Let us now consider a parabola p,

$$x_1 = 0, \quad x_2 - x_3^2 = 0.$$

With arguments as above, we realize that its image $c(p)$ is a parabola. $\Gamma(p)$ is again of class 4, but now it is rational with the ideal plane as double plane. Thus, *the offsets of a parabola are rational of class* 4 (see (Lü, 1994; Farouki and Sederberg, 1995)). This result has been considered as new within the CAGD community, but it follows immediately from the discussion of the cyclographic image curves of arbitrary conics $p \subset \mathbb{R}^3$ (called *hypercycles*) in a paper by W. Blaschke (1910). With the arguments above, we see that the image curves $c(p)$ of arbitrary parabolas p are rational curves with rational offsets and in general of class 4. Later we will return to this example.

2.2. *Bisectors, medial axis and geometrical optics*

A pair of oriented curves c_1, c_2 can be interpreted as cyclographic image of a curve $p \subset \mathbb{R}^3$; p is the intersection of the γ-developables passing through c_1 and c_2. The top view p' of p is usually called (untrimmed) *bisector* or *Voronoi curve* of c_1 and c_2 (Farouki and Johnstone, 1996; Hoffmann, 1992; Pillow, 1995; Choi et al., 1996, 1997). Its points are centers of cycles tangent to c_1 and c_2 and therefore possess equal orthogonal distance to these curves (Fig. 2).

Let $D \subset \mathbb{R}^2$ be a connected domain, bounded by C^2 curves c_i, $i = 1, \ldots, N$. The curves shall be oriented such that the domain lies on the left side. We can then pass the

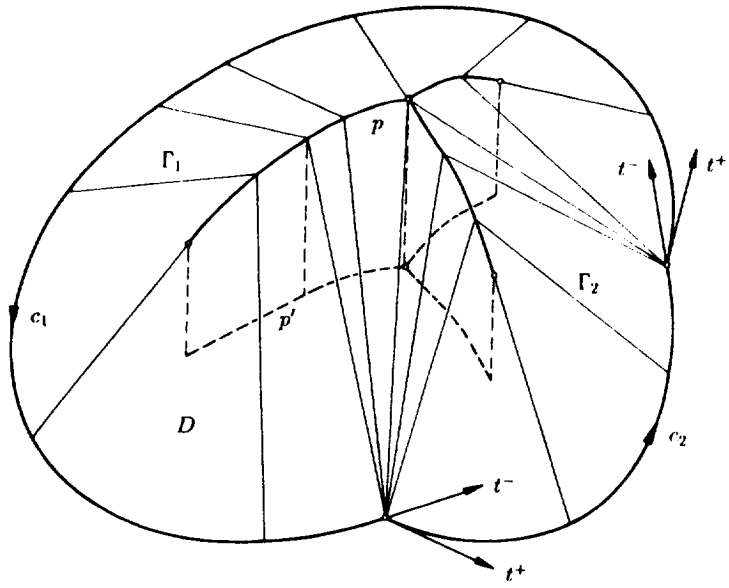

Fig. 4. Computing the medial axis transform.

γ-developables Γ_i through the curves c_i and construct their intersections as well as self-intersections. This results in the untrimmed *medial axis transform* p, which may have several components; its projection p' is the untrimmed *medial axis*. The cyclographic interpretation shows that the medial axis (transform) or bisectors may be computed with surface/surface intersection algorithms (Fig. 4; see also Hoffmann, 1992). To be consistent with the usual definitions (Patrikalakis and Gursoy, 1990; Wolter, 1992), parts of p and p' have to be trimmed off. Only those points of p have to be kept that correspond to maximal cycles in D. This requires to take only points $x' \in p'$ that lie in D and where the radius of $c(x)$ shows the minimal distance from x to the boundary of D. This can easily be done with a *visibility algorithm* as follows. Due to our orientation of the boundary, the interesting parts of p lie in the positive half space H^+: $x_3 \geqslant 0$ of $\mathbb{R}^3$. Projecting the surface $\Gamma^+ = (\bigcup \Gamma_i) \cap H^+$ with projection rays parallel to $(0,0,1)$ onto $\mathbb{R}^2$, exactly the visible parts of the untrimmed curve p, which project into D, form the trimmed medial axis transform p and medial axis p', respectively (Fig. 4).

Discrete curvature discontinuities in the boundary do not cause a problem, but in practice, the boundary may have *tangent discontinuities*. At such a discontinuity with oriented tangents t^-, t^+, one has to introduce a one parameter set of oriented tangents generated by the shortest rotation ρ from t^- into t^+. The γ-developable then contains a part of a γ-cone and the medial axis is computed correctly. If one is just interested in the trimmed medial axis, only 'concave' vertices (those to a negative rotation angle of ρ) have to be filled with a conical part.

As a further simple example for the use of the cyclographic concept we study cusps of the untrimmed medial axis (or bisector). An intersection point x of the γ-developables Γ_i

through the curves c_i is regular if the tangent planes at x are different and if x is regular for both surfaces. An identical tangent plane at x implies a common generator g (γ-line through x) of the developables. Then, there exists a self-tangency in the boundary of D. Two segments of it possess a common oriented line element (x_1, t_1) and the projection g' of g is as common normal at x_1 a component of p'. A higher order analysis would be necessary to decide whether another branch of p has a singularity at g. The remaining singularities stem from intersection points x which lie on the edge of regression e_i of a developable Γ_i; x' is an extraordinary point, if x is a singular point of the curve e_i (corresponding to a curvature extreme of c_i). Hence, *cusps or extraordinary points of the untrimmed medial axis p' lie on the evolutes e_i' of the boundary curves c_i* (see (Farouki and Johnstone, 1996) for the bisector of a point and a curve). *The trimming algorithm, however, eliminates cusps.* This follows from the fact that the osculating circle at a point x_1 of the boundary of D, which is not a curvature extreme, does not lie entirely in D.

Given the medial axis transform p of a domain D, the boundary of D can be reconstructed as $c(p)$. Therefore, the medial axis is sometimes used for shape representation. It is also very useful for the construction of trimmed interior offsets, which are needed for NC pocket machining or layered manufacturing. To construct the interior offset at distance d of the boundary of D we can perform the translation $p_d = p - (0, 0, d)$, and map the part in the positive halfspace, i.e., $p_d \cap H^+$, with c onto $\mathbb{R}^2$.

To obtain an appropriate representation for CAD/CAM purposes, one may compute the medial axis transform from any initial representation of the boundary of D. Then, the medial axis transform can be approximated with a *pe circular spline* (see Section 2.4), which implies that the boundary and all offsets are *circular splines* and the trimming can be performed fast and exactly. One has better approximation properties if a *polynomial quadratic spline* is used to represent the medial axis transform. Trimming the offsets is again efficient and exact; according to Example 2.2, the domain boundary and its offsets are C^1 *rational splines of class* 4 (*and order* 6 *in general*).

The cyclographic mapping of curves possesses a simple, well-known relation to certain problems in *geometrical optics*. Consider a point $x \in p$ with hyperbolic tangent t. Then, the construction of the cyclographic image (Fig. 2) shows that the tangent t' at x' forms equal angles with the lines $x'x_1$ and $x'x_2$. The latter two lines are normals of $c(p)_1$ and $c(p)_2$, respectively. Let us now view the normals of $c(p)_1$ as *light rays* and p' as *mirror*. The angle property shows that the reflected lines are the normals of $c(p)_2$. Any curve, orthogonal to the reflected lines, in particular $c(p)_2$ is called *anticaustic*. The envelope of the reflected rays is the *caustic*. In our spatial interpretation, the caustic is the top view of the edge of regression of the γ-developable through $c(p)_2$.

We obtain *parallel light rays*, if $c(p)_1$ is a line. The γ-developable through $c(p)_1$ is a γ-plane; it contains p. For a *point as light source*, p must lie in a γ-cone. This yields a simple construction of the mirrors to a given system of reflected light rays (Müller and Krames, 1929). One constructs a curve k of constant slope γ whose top view is the given caustic k'. For $k' = (x_1(t), x_2(t))$, we get $k = (x_1(t), x_2(t), s(t))$ with $s(t)$ as arc length function. Then we form the tangent surface $T(k)$ of k. The top view p' of the intersection p of $T(k)$ with any γ-cone $\Gamma(a)$, whose vertex a projects onto the given light source a', is a mirror that generates the given caustic. Analogously, all mirrors for parallel projection are top views of intersections of the same developable $T(k)$

with γ-planes. Replacing reflection by *refraction* according to Snellius' law, mirrors for central or parallel illumination are top views of intersections with cones or planes whose inclination angle against $\mathbb{R}^2$ is different from $\gamma = \pi/4$ (see (Müller and Krames, 1929, pp. 272–275)).

2.3. Canal surfaces as cyclographic images of curves in $\mathbb{R}^4$

A curve $p \subset \mathbb{R}^4$ is mapped by c onto a one-parameter set of spheres $\{c(x),\ x \in p\}$, whose envelope is a *canal surface* and will simply be denoted by $c(p)$. The locus of the cycle centers, i.e., the orthogonal projection p' of p onto $\mathbb{R}^3$ is called its *spine curve*.

For a hyperbolic line p, the surface $c(p)$ is a *cone of revolution* with vertex $s = p \cap \mathbb{R}^3$ and axis p', in particular a *cylinder of revolution* if p is parallel to $\mathbb{R}^3$. The image of a line element (x, p) may be defined as the circle along which the cycle $c(x)$ touches $c(p)$. The points on a parabolic line map to cycles through a common oriented surface element (s, τ) with $s = p \cap \mathbb{R}^3$ and p' as normal of the tangent plane τ. An elliptic line does not possess a real image surface $c(p)$.

A curve with only hyperbolic tangents possesses a real image surface. Hyperbolic segments with parabolic boundary tangents correspond to closed images. Thus, an arbitrary curve p may yield a canal surface with several closed real components corresponding to the hyperbolic segments on p.

A curve p all whose tangents are parabolic (also called γ-curve) is mapped to a one parameter family of cycles each of which touches a surface element determined as image of a tangent of p. The surface elements form a curve s (intersection of the tangent surface $T(p)$ with $\mathbb{R}^3$) with a tangent plane at each curve point. This is called a surface strip. Since the normals of the strip are the projections of the tangents of p, they form a developable surface. Therefore the strip is a so-called *principal curvature strip*. Each surface through the strip possesses the strip curve s as a principal curvature line. The cycles $c(x)$ to points $x \in p$ are centered at the corresponding principal curvature centers.

For CAD applications, *rational canal surfaces* are particularly useful since they may be represented in the standard NURBS form. The cyclographic images of rational curves in $\mathbb{R}^3$ are in general not rational. We will prove in (Peternell and Pottmann, 1997a) the following surprising result (see also (Lü, 1995; Peternell and Pottmann, 1997b)) as a special case of a more general theorem on envelopes of natural quadrics.

Theorem 2.1. *Any canal surface, which is a real component of the cyclographic image of a rational curve in $\mathbb{R}^4$, possesses a real rational parametrization.*

Let us now consider a rational curve segment $p(t)$ in $\mathbb{R}^4$, with hyperbolic tangents only, and represented in rational Bézier form. It may have Bézier points $b_0, \ldots, b_m$ and weights $w_0, \ldots, w_m$. The weights may be replaced by frame points $f_0, \ldots, f_{m-1}$, see (Farin, 1994).

Constructions for the curve $p \subset \mathbb{R}^4$ can now be transferred into $\mathbb{R}^3$ with help of the cyclographic map.

First of all, we obtain a *natural control structure for rational canal surfaces*, consisting of *control cycles* $B_0 = c(b_0), \ldots, B_m = c(b_m)$ and weights (or frame cycles F_i). Note

that in typical CAGD applications, we will not be interested in a canal surface with singular points (corresponding to a sign change of the radius of inscribed cycles) and therefore it will be sufficient to use just control spheres.

Since b_i, f_i, b_{i+1} are collinear, consecutive cycles B_i, F_i, B_{i+1} are inscribed to a common cone of revolution Γ_i. The characteristic end circles of $c(p)$ to $t = 0, 1$ are the circles of contact of B_0, Γ_0 and B_m, Γ_{m-1}, respectively. The convex hull property of p reads as follows.

Proposition 2.2. *A rational canal surface with control cycles $B_0, \ldots, B_m$ and positive weights lies in the convex hull of the control spheres.*

To translate the variation diminishing property, we consider a γ-hyperplane E in $\mathbb{R}^4$. Its points map to cycles which are tangent to the oriented plane $c^*(E)$. We also consider a hyperplane parallel to $\mathbb{R}^3$; the image cycles of its points share the same radius. To formulate the result, it is convenient to define a *complete control structure* of a rational canal surface $c(p)$ as the union of those cycles which are images of points of the control polygon of p.

Proposition 2.3. *Consider the family F of inscribed cycles of an oriented rational canal surface $c(p)$, its complete control structure C and an oriented plane e. Further, assume that $c(p)$ possesses positive weights only. Then, the number of cycles in C that touch e is an upper bound for the number of cycles in F touching e. The number of cycles in C with radius r is greater or equal than the number of cycles in F with radius r.*

The result can be generalized by considering other hyperplanes H in $\mathbb{R}^4$. Their points map to cycles that form the same (not necessarily real) angle with the hyperplane $s := H \cap \mathbb{R}^3$.

2.4. Modeling canal surfaces with Dupin cyclides

The ideas in the previous subsection can nicely be applied to study a class of canal surfaces, which has received much attention within CAGD, namely *Dupin cyclides* (see, e.g., (Albrecht and Degen, 1997; Boehm, 1990; Martin, 1982; Pratt, 1990, 1995; Srinivas and Dutta, 1994, 1995)). A detailed description and new algorithm to construct parametrizations of curves and surface patches on Dupin cyclides is given by Mäurer (1996, 1997). As we will see, the new control structure is very useful for modeling canal surfaces with pieces of Dupin cyclides.

A Dupin cyclide may be defined as envelope of cycles that touch three given cycles A_1, A_2, A_3. Hence, it is the cyclographic image of the intersection curve of the three γ-cones Γ_i with vertices $\zeta(A_i)$. The intersection of two γ-cones Γ_i, Γ_j consists of the quadric Ω at infinity and a quadric in a hyperplane $H_{ij} \subset \mathbb{R}^4$. Therefore, p may also be obtained as intersection of one γ-cone, say Γ_1, with the plane $H_{12} \cap H_{23} \cap H_{13}$. Such a conic is referred to as a *pe circle*, since its ideal points (not necessarily real) lie in Ω.

The pe circle p may be an ellipse, a parabola or a hyperbola. A parabola is mapped to a *parabolic cyclide*, which is a cubic algebraic surface. An ellipse p and a hyperbola p with hyperbolic tangents corresponds to a cyclide of order 4. The usual finer classification is

not invariant under Laguerre transformations; it depends on the singularities of the surface and therefore on the number of intersection points of p and $\mathbb{R}^3$ (see, e.g., (Müller and Krames, 1929, pp. 426–432)).

From now on we exclude those pe circles that are hyperbolas with elliptic tangents. The remaining types of pe circles yield real cyclides. All tangents of p are hyperbolic. Let us now consider a segment p with Bézier points b_0, b_1, b_2. Since p is pe circle the pe distances b_0b_1 and b_1b_2 are equal, i.e.,

$$\langle b_1 - b_0, b_1 - b_0\rangle_{pe} = \langle b_2 - b_1, b_2 - b_1\rangle_{pe}.$$

Therefore, the Bézier cycles B_0B_1 and B_1B_2 of the cyclide piece $c(p)$ possess equal tangential distance. The tangent of p parallel to b_0b_2 contains frame points f_0, f_1 and touches p at the midpoint m of f_0, f_1. Using equality of the pe distances b_0f_0 and f_0m, we find that f_0 divides b_0b_1 in the ratio $w_1 : 1$, where w_1 is the weight of the inner control point b_1 ($w_0 = w_2 = 1$) and computed as

$$w_1 = \frac{\langle b_1 - b_0, b_2 - b_0\rangle_{pe}}{\sqrt{\langle b_1 - b_0, b_1 - b_0\rangle_{pe}\langle b_2 - b_0, b_2 - b_0\rangle_{pe}}}. \tag{11}$$

Proposition 2.4. *The cyclographic image of a pe circle with hyperbolic tangents is a Dupin cyclide. It can be defined with three Bézier cycles B_0, B_1, B_2, for which all centers and the radii of two cycles can be prescribed. The third radius follows from the property that the tangential distances of B_0B_1 and B_1B_2 are equal. The weights are $w_0 = w_2 = 1$ and w_1 is computed from $b_i = \zeta(B_i)$ with Eq.* (11).

This result is useful for the construction of *pe circular splines*. Their cyclographic images are *canal surfaces composed of Dupin cyclide pieces.* With the formulae above, one can transfer results on euclidean circular splines (Hoschek, 1992) into pe geometry.

As an example, we investigate *pe biarcs* which yields new insight and new results on their cyclographic images, called *double cyclide blends* (Boehm, 1990). The problem in $\mathbb{R}^3$ reads: given two cones (or cylinders) of revolution Δ_1, Δ_2 and a boundary circle c_1, c_2 on each of them (see Fig. 6), find a smooth blend between c_1 and c_2, composed of two cyclide segments (since one is usually not sufficient). The input data define oriented line elements a_1, t_1 and a_2, t_2 in pe 4-space $\mathbb{R}^4$, which have to be interpolated with a pair of pe circle segments. The tangents are hyperbolic and therefore t_i can be normalized to $\langle t_i, t_i\rangle_{pe} = 1$, $i = 1, 2$. The inner Bézier points of the two pe circular segments shall be $b_1 = a_1 + \lambda_1 t_1$, $b_2 = a_2 - \lambda_2 t_2$. The junction point is denoted by c (Fig. 5).

An admissible pair of inner Bézier points is characterized by

$$\langle b_2 - b_1, b_2 - b_1\rangle_{pe} = (\lambda_1 + \lambda_2)^2.$$

This is equivalent to

$$\begin{aligned}&\langle a_2 - a_1, a_2 - a_1\rangle_{pe} - 2\lambda_1\langle a_2 - a_1, t_1\rangle_{pe} - 2\lambda_2\langle a_2 - a_1, t_2\rangle_{pe}\\ &\quad + 2\lambda_1\lambda_2\big(\langle t_1, t_2\rangle_{pe} - 1\big) = 0.\end{aligned} \tag{12}$$

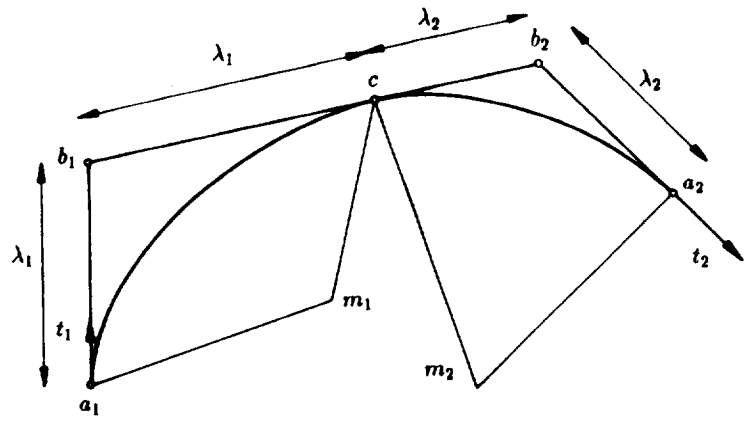

Fig. 5. Bézier points of a pe biarc in $\mathbb{R}^4$.

One may choose b_1 (λ_1) and then formula (12) determines a unique b_2 (λ_2) and the junction point

$$c = \frac{\lambda_2 b_1 + \lambda_1 b_2}{\lambda_1 + \lambda_2}.$$

If $\lambda_i > 0$, one uses the arc contained in the triangle a_i, b_i, c. Otherwise one has to use the complementary arc. The signs of λ_i also define whether c is between b_1 and b_2 or not. The mapping $b_1 \mapsto b_2$ is a *projective map* between the end tangents because of the bilinearity of (12). Therefore the junction tangents $b_1 b_2$ form in general a ruled quadric. If the input data a_1, t_1 and a_2, t_2 span just a plane, we obtain the tangents of a conic or the lines of a pencil (for $t_1 = -t_2$). Inserting relation (12) into the expression for c, we find that the locus of junction points c is a pe circle d. Application of the cyclographic map gives us the following result on the one parameter set of double cyclide blends.

Proposition 2.5. *Given two cones or cylinders of revolution Δ_1, Δ_2 with a boundary circle c_1, c_2 on each of them, there is a one parameter family of double cyclide blends that form a smooth join of the given surfaces between c_1 and c_2. The junction circles of the cyclide pairs lie in a Dupin cyclide, the cyclographic image of the pe circle d. The axes of the junction circles are contained in a family of generators of a ruled quadric, the tangents of a conic or the lines of a pencil.*

If the input data in $\mathbb{R}^4$ lie in a plane α, which happens if the axes of the two given cones or cylinders in $\mathbb{R}^3$ are coplanar, also the solution biarcs lie in α. Corresponding to the γ-hyperplanes passing through α in $\mathbb{R}^4$, the image cycles of points in α touch 2 planes, one plane along a line or 2 conjugate complex planes (see Section 2.5). The same is true for the surfaces in the possible double-cyclide blends.

Let us now assume that the data span a hyperplane H ('spatial data'). If H is a γ-hyperplane, its points are mapped to cycles that touch the plane $c^*(H)$. Otherwise, the projective extension of H intersects the absolute quadric Ω in a real or imaginary conic

and we speak of a *pseudoeuclidean* or *euclidean hyperplane*, respectively. The points of a pe H are mapped to cycles intersecting the plane $h := H \cap \mathbb{R}^3$ in a fixed angle. For a euclidean H, the image cycles are such that any two of them define a connecting cone of revolution whose vertex lies in $h := H \cap \mathbb{R}^3$. Note that h is determined by the vertices of the input cones Δ_i and by the vertex of the cone connecting the two cycles C_i which touch Δ_i along c_i. The type of H depends on the type of $h \cap C_i$ which shows that all three types of H may occur in applications. It can be shown that the pe biarcs lie in a *pe 2-sphere* $\Sigma \subset H$, i.e., the intersection quadric of a γ-cone with H. Its points map to cycles touching 2 cycles or a cycle and a plane in the case of a γ-hyperplane H (see Example 2.3).

Proposition 2.6. *All double cyclide blends from Proposition* 2.5 *for skew axes of the input cones* Δ_i *are in line contact with two fixed cycles* C_1, C_2, *one of which may degenerate to a plane.* C_1, C_2 *are exactly those cycles or planes which touch the input cones* Δ_i *at points of the boundary circles* c_i.

A euclidean hyperplane H can be transformed with a pe similarity into $\mathbb{R}^3$. This pe similarity describes a Laguerre transformation which maps both data cones Δ_i to lines and the double cyclide blends to euclidean circular biarcs. Therefore, in the case of 'euclidean input data' our results are Laguerre geometrically equivalent to those in (Fuhs and Stachel, 1988).

Practically useful double cyclide blends have to be free of singularities. This means that the pe biarc in $\mathbb{R}^4$ should not intersect $\mathbb{R}^3$. Moreover, it seems to be desirable that the blend does not possess an unnecessarily large variation in the radius of the inscribed spheres. We therefore propose to construct a *double-cyclide blend with minimal radial variation* as follows. In view of the properties of the control structure, one can measure

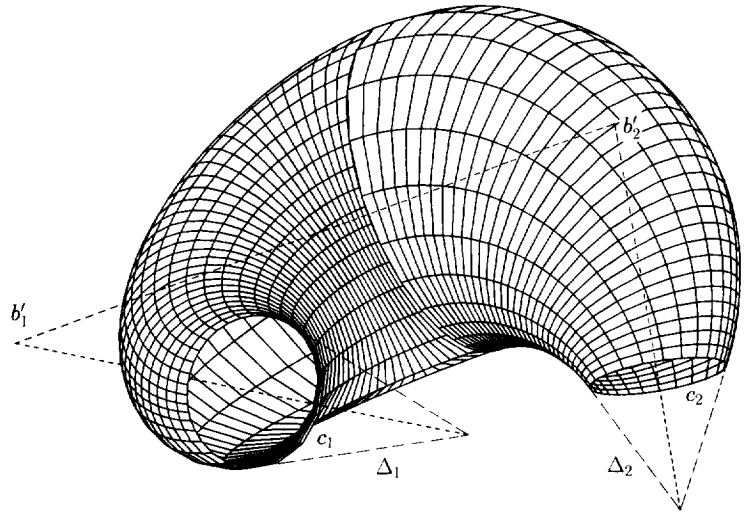

Fig. 6. Double cyclide blend with minimum radial variation.

the *radial variation* ρ by the radial variation in the spheres of the complete control structure and define

$$\rho := \lambda_1^2 t_{1,4}^2 + \lambda_2^2 t_{2,4}^2, \tag{13}$$

with $t_i = (t_{i,1}, \ldots, t_{i,4})$, $i = 1, 2$. Rewriting (12) in the form

$$\lambda_2 = \frac{\alpha\lambda_1 + \beta}{\gamma\lambda_1 + \delta},$$

the λ_1-value to the minimum satisfies

$$t_{1,4}^2 \lambda_1 (\gamma\lambda_1 + \delta)^3 + t_{2,4}^2 (\alpha\delta - \beta\gamma)(\alpha\lambda_1 + \beta) = 0. \tag{14}$$

An example of a blend with minimum radial variation in this sense is shown in Fig. 6. It is, however, not guaranteed that this solution is free of singularities and there might be no regular solution at all. Then, one can work with more than two cyclide pieces.

Remark 2.1. *Let p, q be two curves in $\mathbb{R}^4$ which possess contact of order $d \geqslant 1$ at a point $x \notin \mathbb{R}^3$ with hyperbolic tangent t. Then, the canal surfaces $c(p), c(q)$ also meet with contact of order d along a circle k which corresponds to the line element (x, t).*

In particular, if x is an inflection point, the *osculating tangent line* is mapped to an osculating cone of revolution. Otherwise the *osculating pe circle* q at $x \in p$ is mapped to an *osculating cyclide* of the canal surface $c(p)$. The parabolic points (points with vanishing Gaussian curvature) of the cyclide $c(q)$ lie in the planes which form the image $c(s)$

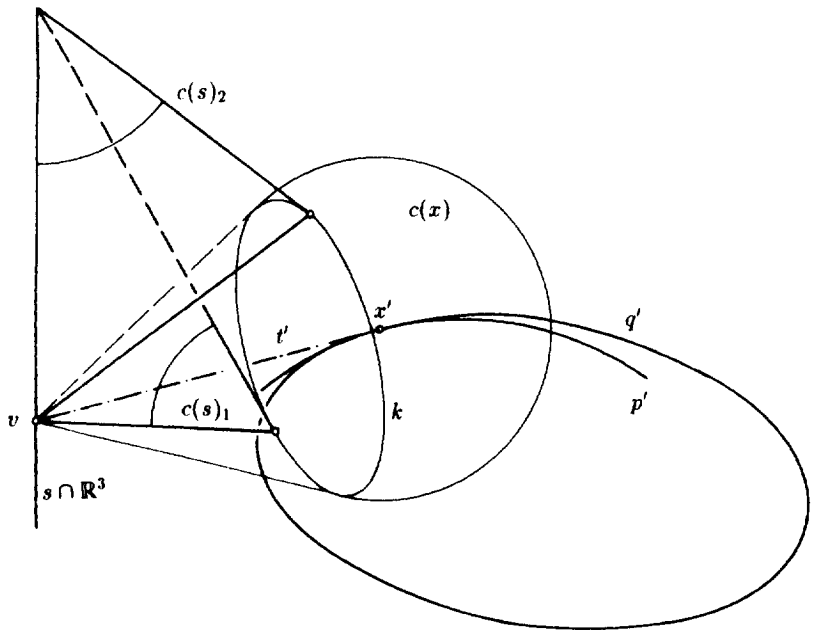

Fig. 7. Constructing parabolic points of a canal surface.

of the osculating plane $s \supset q$ (see Section 2.5). The line $s \cap \mathbb{R}^3$ lies in $c(s)$ and contains the vertices of all circumscribed cones of the cyclide $c(q)$. In particular $s \cap \mathbb{R}^3$ contains the vertex $v = t \cap \mathbb{R}^3$ of the cone $c(t)$ that touches $c(p)$ along k. Let V be the locus of vertices of all circumscribed cones of the canal surface $c(p)$. Then $s \cap \mathbb{R}^3$ is tangent to V in v. This yields a simple construction of the parabolic points of a characteristic circle k of a canal surface illustrated in Fig. 7. From that we get information on the behavior of canal surfaces $c(p)$ to G^1 curves $p \subset \mathbb{R}^4$ with continuous osculating planes.

2.5. *Cyclographic mapping of surfaces in* $\mathbb{R}^4$ *and some applications*

The cyclographic mapping of surfaces in $\mathbb{R}^4$ did not receive so much attention in the classical literature as cyclographic images of curves in $\mathbb{R}^3$. On the other hand, surfaces are a much more active research area in geometric design than curves. Therefore we describe the surface case in some detail, although there are clearly many analogies to the lower dimensional curve case.

Let $s(u, v)$ be a real C^1 surface $\subset \mathbb{R}^4$. Applying the cyclographic map c, we get a two parameter set of cycles $c(s(u, v))$ possessing a real or imaginary envelope $c(s)$ which may consist of several sheets.

It is good to begin with a plane s. The ideal line of s contains 0, 1 or 2 real points of the pe absolute quadric Ω; we speak of a *euclidean, isotropic* or *pseudoeuclidean plane*, respectively.

For a euclidean plane s, $c(s)$ contains two real (oriented) planes $c(s)_1 = s_1$, $c(s)_2 = s_2$. For each $x \in s$, the planes s_1, s_2 are tangent to the cycle $c(x)$ at points x_1, x_2. We call the oriented surface elements (x_1, s_1) and (x_2, s_2) the *cyclographic image of the surface element* (x, s). The planes s_1 and s_2 are the intersections (c^* images) of the γ-hyperplanes

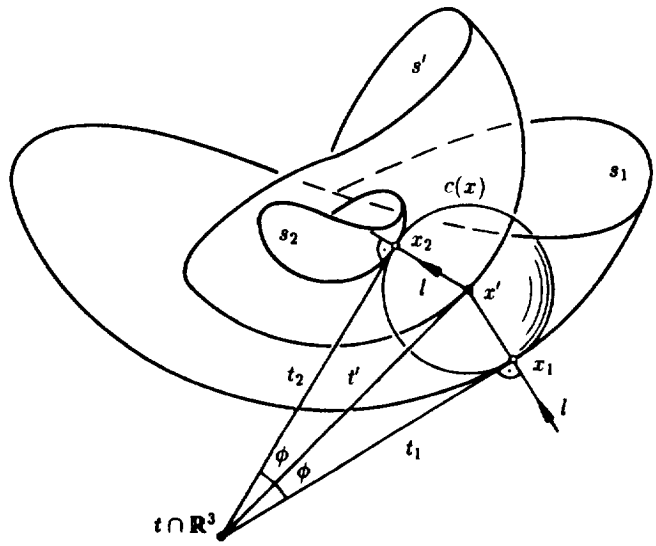

Fig. 8. Cyclographic image of a surface and optical interpretation.

through s with the reference space $\mathbb{R}^3$. Clearly, the intersection of s_1 and s_2 is the line $s \cap \mathbb{R}^3$.

If s is an isotropic plane (also called γ-plane), all image cycles of points in s touch an oriented plane e (orthogonal to the projection s') at points of the line $s \cap \mathbb{R}^3$. Any point x in s determines just one surface element (x_1, e). The envelope $c(s)$ to a pe plane s is not real.

For general surfaces s, we proceed as above and map its surface elements (x, t), where t is the tangent plane at $x \subset s$ (Fig. 8).

A particular discussion is necessary for the case of a surface s all whose tangent planes are isotropic; we call it a γ-surface. At each of its points, there is a unique parabolic surface tangent. Integrating this field of γ-tangents we obtain a family of γ-curves on s. Their cyclographic images are principal curvature strips on the image surface $c(s)$. The projection s' of s is locus of principal curvature centers, i.e., a sheet of the focal surface of $c(s)$. The surface $c(s)$ possesses a second sheet of the focal surface corresponding to the other family of principal curvature lines. The γ-tangents of s form a *γ-hypersurface* $T(s)$ in $\mathbb{R}^4$, which may also be considered as cyclographic preimage of all cycles touching the oriented surface $c(s)$ or as graph of the signed distance function to the surface $c(s)$. The surface s consists of singular points of $T(s)$. All intersections of $T(s)$ with hyperplanes H parallel to $\mathbb{R}^3$ are translates of the offsets of $c(s)$ and possess edges of regression at $s \cap H$. This yields the well-known fact that edges of regression of the offsets to a surface lie on its focal surface.

The cyclographic mapping of a general surface $s \subset \mathbb{R}^4$ can now be formulated as follows: *pass the γ-hypersurfaces $\Gamma(s)$ through s and intersect them with $\mathbb{R}^3$. For a surface s with only euclidean tangent planes, $c(s)$ consists of* 2 *sheets, a γ-surface is mapped to a single surface sheet and a surface with only pseudoeuclidean tangent planes possesses no real image surface $c(s)$.*

Consider two surface patches $s_1, s_2 \subset \mathbb{R}^4$ joined along a curve p. If the joint is just C^0, the image surfaces $c(s_1)$ and $c(s_2)$ are joined smoothly by (the appropriate parts of) the canal surface $c(p)$. In this sense, the *cyclographic map automatically generates blends.* A G^k surface $s_1 \cup s_2$ yields a G^k cyclographic image.

Example 2.3. Let s be a 2-dimensional pe sphere, i.e., the intersection of a hyperplane H with a γ-cone $\Gamma(a)$. For a γ-hyperplane H, the complete γ-surface through s is $H \cup \Gamma(a)$ and therefore $c(s)$ is a *cycle* $\Gamma(a) \cap \mathbb{R}^3$ and an *or. plane* $H \cap \mathbb{R}^3$. Otherwise, there exists a pe reflection σ at H which maps $\Gamma(a)$ to a second γ-cone $\Gamma(\sigma(a))$ through s. The cyclographic image $c(s)$ is the *union of two cycles* $c(a)$ and $c(\sigma(a))$, the intersections of $\Gamma(a)$ and $\Gamma(\sigma(a))$ with $\mathbb{R}^3$. A 'polyhedral' surface s with pe spherical faces and pe circle segments as edges has a smooth cyclographic image $c(s)$ consisting of spherical 'face patches' blended by cyclide patches as 'edge fillets' and spherical 'corner patches'. Convex surfaces of this kind have been modeled by Gallagher and Piper (1994) with a Möbius geometric approach.

A pair of oriented surfaces s_1, s_2 in $\mathbb{R}^3$ may be considered as cyclographic image of a surface s in $\mathbb{R}^4$, which is the intersection of the γ-hypersurfaces through s_i. The projection s' of s is the untrimmed *bisector* or *Voronoi surface* of s_1, s_2. A connected

domain D with boundary surfaces s_i determines γ-hypersurfaces whose intersections and self-intersections form the untrimmed *medial axis transform* of D; s' is the untrimmed *medial axis* or *skeleton*. As in the curve case, the computation of an untrimmed bisector or medial axis (transform) is now formulated as an intersection problem in $\mathbb{R}^4$. However, in contrast to surface/surface intersection in 3-space, this problem has not yet received much attention. We also see that *cuspidal edges of the untrimmed medial axis lie on the focal surfaces of the boundary of* D. The trimming procedure is again formulated with a visibility algorithm. Voronoi surfaces of polyhedra have been treated with the present geometric method by Stachel and Abdelmoez (1992).

Let $x \in s$ be a point with euclidean tangent plane t. Then, the cyclographic image of the surface element (x, t) consists of two surface elements with points x_1 and x_2. The normals of these elements are $x'x_1$ and $x'x_2$, which form the same angle with the tangent plane t' to s' at x' (Fig. 8). Therefore, we can now formulate an analogous *optical interpretation* as in the curve case. Considering the normals of $c(s)_1 = s_1$ as light rays, $c(s)_2 = s_2$ is a reflectional anticaustic to the mirror s'. If the surface s lies in a γ-hyperplane or a γ-cone, we obtain parallel light rays or a central illumination, respectively.

Note the relation between the construction of anticaustics in the case of parallel light rays (orthogonal to a plane, say a) and the transformation Λ^* from the standard model of Laguerre space to its dual isotropic model. An anticaustic for the given illumination to a mirror surface s' (interpreted as set of tangent planes) is obtained as $(\Lambda^*)^{-1}(s')$ and easily computed with (10). Clearly, the same holds in the planar case.

Acknowledgements

This research has been supported by the Austrian Science Foundation through project P09790.

References

Albrecht, G. and Degen, W.L.F. (1997), Construction of Bezier rectangles and triangles on the symmetric Dupin horn cyclide by means of inversion, Computer Aided Geometric Design 14, 349–375.

Benz, W. (1992), *Geometrische Transformationen*, BI-Wiss.-Verlag, Mannheim.

Blaschke, W. (1910), Untersuchungen über die Geometrie der Speere in der Euklidischen Ebene, Monatshefte für Mathematik und Physik 21, 3–60.

Blaschke, W. (1929), *Vorlesungen über Differentialgeometrie III*, Springer, Berlin.

Boehm, W. (1990), On cyclides in geometric modeling, Computer Aided Geometric Design 7, 243–255.

Bruce, J.W., Giblin, P.J. and Gibson, C.G. (1985), Symmetry sets, Proc. Roy. Soc. Edinburgh 101A, 163–186.

Cecil, T.E. (1992), *Lie Sphere Geometry*, Springer, Berlin, Heidelberg, New York.

Choi, H.I., Choi, S.W. and Moon, H.P. (1996a), Mathematical theory of medial axis transform, RIM–GARC Preprint Series 95–87, Seoul National University.

Choi, H.I., Choi, S.W. and Moon, H.P. (1996b), New algorithm for medial axis transform of plane domain, RIM–GARC Preprint Series 95–88, Seoul National University.

Choi, J.J., Kim, M.S. and Elber, G. (1997), Computing planar bisector curves based on developable SSI, submitted to Computer Aided Design.

Farin, G. (1994), *NURBS for Rational Curve and Surface Design*, AK Peters, Wellesley, MA.

Farouki, R.T. and J.-C. A. Chastang (1992), Curves and surfaces in geometrical optics, in: Lyche, T. and Schumaker, L.L., eds., *Mathematical Methods in Computer Aided Geometric Design II*, Academic Press, 239–260.

Farouki, R.T. and Johnstone, J. (1996), Computing point/curve and curve/curve bisectors, in: Fisher, R., ed., *The Mathematics of Surfaces V*, Oxford University Press.

Farouki, R.T. and Sederberg, T. (1995), Analysis of the offset to a parabola, Computer Aided Geometric Design 12, 639–645.

Farouki, R.T. et al. (1994), Offset curves in layered manufacturing, ASME PED-Vol. 68-2, Manufacturing Science and Engineering Book No. G0930B, 557–568.

Fuhs, W. and Stachel, H. (1988), Circular pipe connections, Computers & Graphics 12, 53–57.

Gallagher, T. and Piper, B. (1994), Convexity preserving surface interpolation, in: Sapidis N.S., ed., *Designing Fair Curves and Surfaces*, SIAM, Philadelphia, 161–209.

Hoffmann, C.M. (1992), Computer vision, descriptive geometry and classical mechanics, in: Falcidieno, B., Hermann, I. and Pienovi, C., eds., *Computer Graphics and Mathematics*, Springer, Eurographics Series, 229–244.

Hoschek, J. (1992), Circular splines, Computer Aided Design 24, 611–618.

Hoschek, J. and Lasser, D. (1993), *Fundamentals of Computer Aided Geometric Design*, AK Peters, Wellesley, MA.

Lü, W. (1994), Rationality of the offsets to algebraic curves and surfaces, Applied Mathematics (Journal of Chinese Universities) 9 (Ser. B), 265–278.

Lü, W. (1995), Rational canal surfaces, Technical Report Nr. 26, Institut für Geometrie, TU Wien.

Martin, R.R. (1982), Principal patches for computational geometry, PhD Thesis, Cambridge University.

Mäurer, Ch. (1996), Rational curves and surfaces on Dupin ring cyclides, Preprint Nr. 1806, Fachbereich Mathematik, TH Darmstadt.

Mäurer, Ch. (1997), Rationale Bézier-Kurven und Bézier-Flächenstücke auf Dupinschen Zykliden, Dissertation, TH Darmstadt.

Müller, E. and Krames, L. (1929), *Vorlesungen über Darstellende Geometrie II*, Deuticke, Leipzig und Wien.

Patrikalakis, N.M. and Gursoy, H.N. (1990), Shape interrogation by medial axis transform, in: Ravani, B., ed., *Advances in Design Automation, Computer Aided and Computational Design*, Vol. 1, ASME, Chicago, 77–88.

Peternell, M. and Pottmann, H. (1997a), A Laguerre geometric approach to rational offsets, Computer Aided Geometric Design, to appear.

Peternell, M. and Pottmann, H. (1997b), Computing rational parametrizations of canal surfaces, J. Symbolic Computation 23, 255–266.

Pillow, N., Utcke, S. and Zisserman, A. (1995), Viewpoint-invariant representation of generalized cylinders using the symmetry set, Image and Vision Computing 13, 355–365.

Pratt, M.J. (1990), Cyclides in computer aided geometric design, Computer Aided Geometric Design 7, 221–242.

Pratt, M.J. (1995), Cyclides in computer aided geometric design II, Computer Aided Geometric Design 12, 131–152.

Srinivas, Y.L. and Dutta, D. (1994), An intuitive procedure for constructing geometrically complex objects using cyclides, Computer Aided Design 26, 327–335.

Srinivas, Y.L. and Dutta, D. (1995), Rational parametric representation of parabolic cyclide: Formulation and applications, Computer Aided Geometric Design 12, 551–566.

Stachel, H. and Abdelmoez, H. (1992), Voronoi diagrams and offsets, an algorithm based on descriptive geometry, in: *Proceedings Compugraphics '92*, Lisbon, Portugal, 159–166.

Wolter, F.E. (1992), Cut locus and medial axis in global shape interrogation and representation, MIT, Dept. of Ocean Engineering, Design Laboratory Memorandum 92-2.